Fabrication tolerance of asymmetric silicon-on-insulator polarization rotators

Henghua Deng

Department of Electrical and Computer Engineering, University of Waterloo, Ontario, N2L 3G1, Canada

David O. Yevick

Department of Physics, University of Waterloo, Ontario, N2L 3G1, Canada

Chris Brooks and Paul E. Jessop

Department of Engineering Physics, McMaster University, Hamilton, Ontario, L8S 4L7, Canada

Received June 17, 2005; revised October 28, 2005; accepted January 6, 2006; posted February 3, 2006 (Doc. ID 62879)

We investigate the fabrication tolerance of novel slanted-angle silicon-on-insulator polarization rotators with asymmetric external waveguiding regions. We also minimize the input and output coupling loss between the polarization rotator and the rib waveguides through a lateral shift in the relative waveguide positions. © 2006 Optical Society of America

OCIS codes: 130.3120, 130.2790.

1. INTRODUCTION

Polarization-manipulating devices[1] are key components in optical fiber communication systems. Polarization splitters[2,3] that separate hybrid polarization into transverse-electric (TE) and transverse-magnetic (TM) field components have been realized using structures such as multimode interferometers, Mach–Zehnder interferometers, and Y junctions. Polarization rotators can be more simply constructed from single or multiple sections of asymmetric passive waveguides,[4] although active devices employing electro-optic or thermal strain effects can also be made.[1]

Specializing to passive polarization rotators, in designs based on periodic asymmetrically loaded sections, alternating waveguide junctions are employed to accumulate multiple small rotations[4–6]; however, fabrication difficulties and repeated losses at these junctions limit the utility of such devices to compact photonic integrated circuits. Alternatively, a properly designed single asymmetric waveguide can rotate the optical field by 90°, resulting in a single-section polarization converter.[7–13]

Most reported single-section slanted-angle (angled-facet) polarization converters employ III–V semiconductor rib waveguides with thick substrates. Consequently, the waveguide is single mode only over a relatively small region of waveguide parameters, while the radiation loss into the substrate and hence the coupling loss to single-mode fibers are significant. In addition, the lack of very strong optical confinement leads to enhanced bending losses. This limits the minimum size of devices containing such waveguides and therefore restricts the component density in future high-speed integrated platforms. To decrease optical losses, high-index-contrast materials can be employed. Recently, we therefore developed silicon-on-insulator (SOI) passive polarization rotators.[14–16] Compared with conventional III–V designs, SOI polarization rotators provide improved optical confinement and decreased wavelength sensitivity as well as enhanced fabrication tolerance.[14] Further, they can be integrated with electronic components to enable low-cost, large-scale, and high-density optoelectronic integrated circuits.

In this paper, we consider in detail the fabrication tolerance of two representative single-section SOI polarization rotator designs. In particular, we investigate the performance variations associated with small changes in geometrical parameters such as the rib width, rib height, outer-slab thickness, and the angles of both slanted and vertical sidewalls from their optimal values. We also consider the variation in coupling loss between a polarization-rotating waveguide and standard input and output SOI rib waveguides as a function of the lateral offset between their centers.

2. NUMERICAL MODEL AND GEOMETRIC PARAMETERS

We will consider asymmetric SOI polarization-rotating waveguides with the general form of Fig. 1, where H, W, h, and θ denote the rib height (wafer size), rib width, outer-slab thickness, and the slanted angle, and the refractive indices for Si and SiO_2 are $n_1=3.48$ and $n_2=1.45$. The sloped sidewall is etched completely to the SiO_2 insulator layer along the $\theta=54.736°$ silicon crystal plane, considerably simplifying device fabrication.[14] The height, width, and slab thickness of the input and output SOI rib waveguides are designated by H_{rib}, W_{rib}, and h_{rib}.

1084-7529/06/071741-5/$15.00 © 2006 Optical Society of America

To simplify fabrication, the outer-slab thickness and rib height of the slanted-angle polarization rotator will be taken to coincide with those of the input and output SOI rib waveguides.

Although significant regions in the space of the values of the parameters H, W, and h yield waveguides with complete TE↔TM polarization conversion as detailed in Ref. 14, we here select two representative devices with $(H,W,h)=(4.8,4.8,1.8)$ μm and $(H,W,h)=(2.8,2.7,1.0)$ μm, which we refer to as the 5 μm and 3 μm devices. Employing the full-vectorial finite-element-method eigenmode solver,[17] we find optical axis rotation angles and half-beat lengths of $\varphi=46.12°$, $L_\pi=2572$ μm for the 5 μm device and $\varphi=45.29°$, $L_\pi=502.4$ μm for the 3 μm device. Figure 2 displays the eigenmode distribution of the two fundamental polarizations in the 3 μm device. Clearly, the geometric asymmetry hybridizes the transverse and lateral polarization components so that these become TE and TM with respect to the angled facet rather than with respect to the substrate interface. Since the transverse components of each mode are then almost identically distributed, the optical axis is positioned at $\varphi=45°$ to the lateral direction. As a result, the polarization of an incoming TE or TM mode rotates by 90° after the half-beat length,

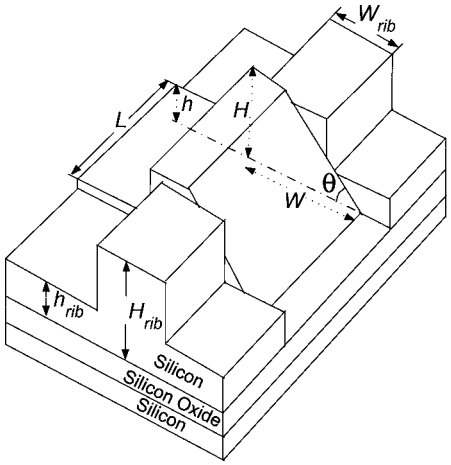


Fig. 1. SOI slanted-angle polarization rotator with an asymmetric external layer butt coupled to input and output SOI rib waveguides.

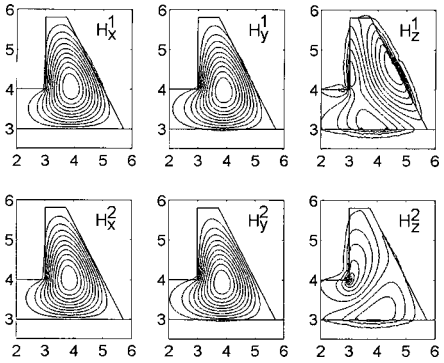


Fig. 2. Lowest-order modal field distributions in the lateral and transverse polarizations of a slanted-angle SOI polarization rotator with $(H,W,h)=(2.8,2.7,1.0)$ μm.

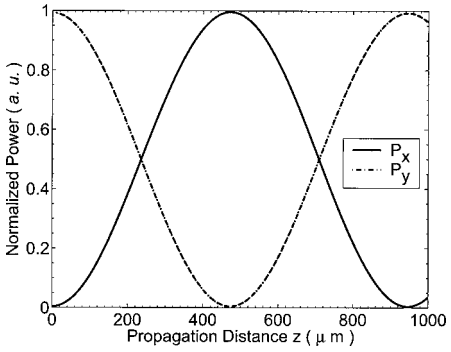


Fig. 3. Power in the TE and TM modes of a 3.0 μm SOI polarization rotator excited by a TE-polarized input.

$$L_\pi=\frac{\pi}{\beta_1-\beta_2}, \tag{1}$$

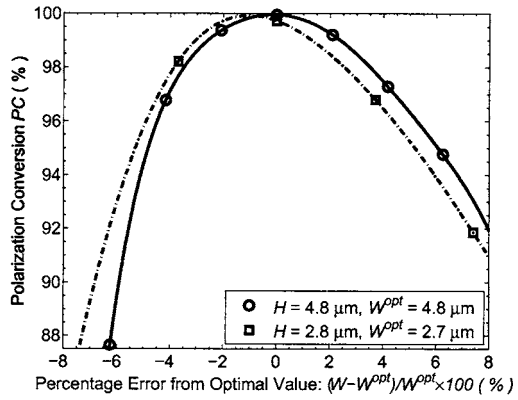
where β_1 and β_2 are the propagation constants of the fundamental polarized modes. The performance of the rotator is thus characterized by the values of the polarization conversion efficiency (PC) and the polarization extinction ratio.[14]

Next, in Fig. 3 we employ a full-vectorial finite-element beam propagation method program with perfectly matched layer boundary conditions[18] to simulate the power in the transverse field components H_x and H_y in the 3 μm SOI polarization rotator excited by a TE-polarized field with the shape of the lowest-order field distribution. In this configuration the TE-polarized input light is converted with a PC of 99.60% into a TM-polarized field with a dominant field H_x after a propagation distance of L_π and is then reconverted into a TE-polarized field with a dominant field H_y after an additional half-beat length. The PC for a TM-polarized input field is calculated as PC=99.61%, which is nearly equal to the TE result, unlike the results for previous III–V periodically loaded asymmetric polarization rotators that show large differences for TE and TM inputs.[4,7]

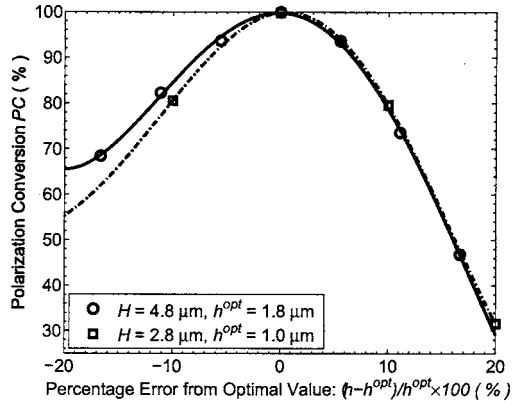
3. FABRICATION TOLERANCE

Variations in operating wavelength and device parameters resulting from manufacturing errors inevitably affect the conversion efficiency of slanted-angle SOI polarization rotators. In a previous work[14] we have demonstrated that the strong optical confinement of SOI polarization converters ensures nearly wavelength-independent operation in the International Telecommunication Union–Telecommunication Standardization Sector's C (1528.77–1563.86 nm) and L(1573.71–1604.03 nm) bands, as required by dense wavelength division multiplexing (DWDM) applications. In this paper, we extend our previous analyses to PC variations induced by possible fabrication errors.

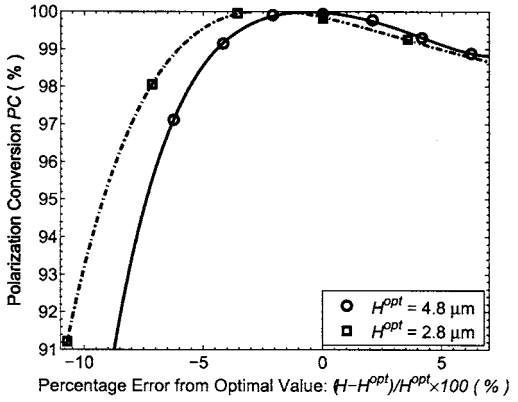
Accordingly, we first examine in Fig. 4 the change in PC as a function of the individual slanted-angle rib waveguide dimensions. To better contrast the behavior of the 3 and 5 μm polarization rotators, the geometric parameters in Fig. 4 are normalized with respect to their silicon guiding layer thicknesses, so that the x axes indicate the relative geometric error. Figure 4(a) illustrates the depen-



(a)



(b)



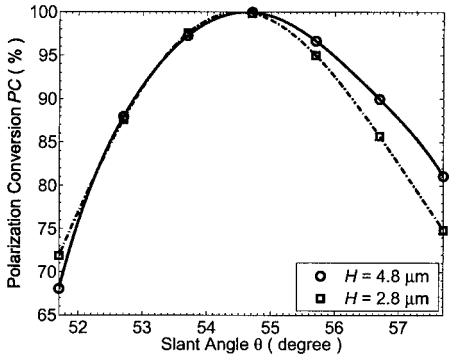
(c)

Fig. 4. Variation of the PC with respect to (a) the base rib width W, (b) the outer-slab thickness h, and (c) the rib height H.

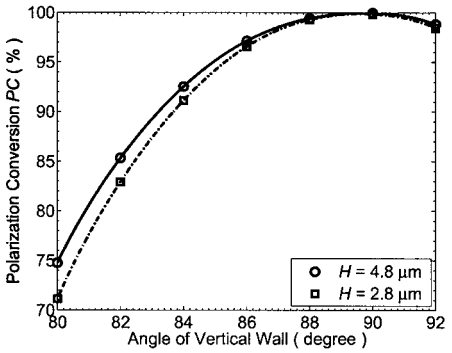
dence of the PC on the base rib width W for these two representative devices. For the 5 μm design, the PC decreases by only 1% for a deviation of ±0.1 μm from the optimum rib width of 4.8 μm, while the corresponding value for the 3 μm design with optimum rib width 2.7 μm is ≈2.5%. Both of these values compare favorably with the results presented in Fig. 5 of Ref. 10 for an InGaAsP slanted-angle polarization converter, for which the PC decreases by 2.5% when the rib width is expanded by 0.1 μm.

In contrast, varying the outer-slab layer thickness h yields the curves of Fig. 4(b), which indicate a larger effect on the device performance. Thus a ±0.1 μm variation of h from its optimal value reduces the PC by 5% for the 5 μm device and by 18% for the 3 μm SOI polarization rotator. For a fabrication tolerance of ±20 nm, however, the performance degradation of the 3 μm device dramatically improves to less than 3%. Figure 4(c) shows the PC variation with respect to changing rib height H. Even when the relative variation of rib height is as large as 10%, the PC is still well above 90%. In general, then, varying any of the parameters H, W, or h by 5% or less reduces the PC by ≤5%, where the largest change results from variations in the outer-slab thickness.

Next, we analyze in Fig. 5 the degradation of the PC with respect to the variation of the angles of both the slanted and the vertical rib sidewalls. We display in Fig. 5(a) the dependence of the PC on the angle of the slanted facet, which is normally 54.736°, corresponding to the etch direction perpendicular to the ⟨111⟩ Si crystal plane. Evidently, a small change of 1° in the slant angle lowers the PC by 3%. However, for wet etching employing, for example, potassium hydroxide or tetramethyl ammonium hydroxide, errors in the slanted angle are negligible.[15] In contrast, angular errors in the vertical wall far more significantly affect the device performance, as illustrated in Fig. 5(b), where a 5° deviation from the right angle reduces the PC by 6% and a 10° deviation leads to a >25% degradation.



(a)



(b)

Fig. 5. Variation of the PC with respect to (a) the angle of the slanted facet θ and (b) the angle of the vertical sidewall.

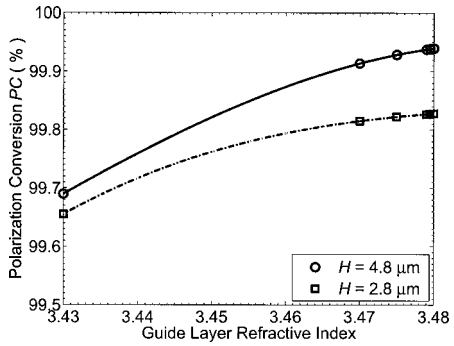


Fig. 6. Variation of the PC with respect to refractive index of the silicon guiding region.

Finally, we analyze in Fig. 6 the dependence of the PC on changes of the refractive index of the silicon guiding film that may, for example, result from unintentional doping. Since these changes are small compared with the refractive index difference between silicon ($n_1=3.48$) and silicon dioxide ($n_2=1.45$), Fig. 6 indicates a minimal effect on device performance. For example, setting the index of the silicon guiding region to 3.43 reduces the PC by only 0.3%. Such a refractive index variation would produce large performance changes in III–V semiconductor polarization converters, which typically require refractive index tolerances of $\Delta n < 0.1$ as a result of the smaller index contrast and hence weaker guiding.[9,10]

4. COUPLING LOSSES

Although several strategies have been proposed for mode conversion between an input or output rib waveguide and a polarization converter, in most photonic integrated circuit applications a polarization converter is directly butt coupled to the input and output rib waveguides, as illustrated in Fig. 1 and the corresponding two-dimensional cross-sectional view in Fig. 7. The centers of the input and output waveguides in the transverse direction, which are characterized by the rib height H_{rib}, rib width W_{rib}, and outer-slab thickness h_{rib}, are here displaced by a transverse distance δ with respect to the center of the slanted-angle polarization converter.

To determine the value of the lateral shift that yields the maximum coupling efficiency between the SOI polarization rotator and the input or output rib waveguides, the overlap between the fundamental modes of the slab and slanted-angle waveguides is repeatedly evaluated for different values of δ. We consider first the most easily fabricated configuration with $H_{rib}=H$ and $h_{rib}=h$ and specialize to the 3 μm design. We select typical values of the rib height and the outer-slab thickness of the input and output rib waveguides, namely, $H_{rib}=2.8$ μm and $h_{rib}=1.0$ μm. Varying the widths of these waveguides W_{rib} from 1.6 to 3.0 μm and the lateral shift δ from -1.0 to 0.0 μm yields the TE and TM two-dimensional coupling loss graphs shown in Fig. 8. From this figure, we conclude that the minimum losses of -0.21 dB for a TE input field and -0.19 dB for a TM input field are obtained for a rib width $W_{rib}=2.0$ μm and a lateral offset of $\delta=-0.6$ μm. Further, $\delta=-0.6$ μm yields the approximate minimum insertion loss for input and output rib widths between 1.6 and 3.0 μm.

If the vertical walls of the SOI rib waveguide and the slanted-angle SOI polarization converter coincide, the minimum coupling loss of 0.2 dB for both polarizations is obtained for the 3 μm design when the rib height $H_{rib}=3.0$ μm and slab thickness $h_{rib}=1.1$ μm are identical for both the rib and the slanted-angle waveguides and the rib width $W_{rib}=2.0$ μm. As a comparison, the total insertion loss for the equivalent III–V converter has been evaluated as 0.5 dB in Ref. 9 and 0.6 dB in Ref. 10. Increasing W_{rib}

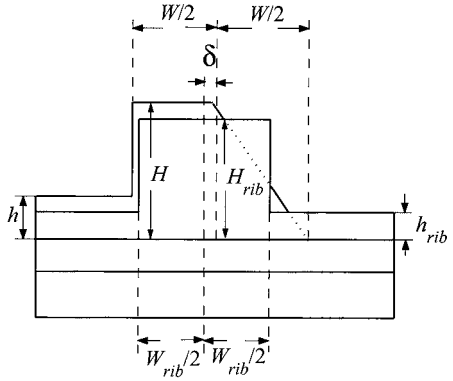


Fig. 7. Cross section of the junction between the SOI polarization rotator and the input and output rib waveguides.

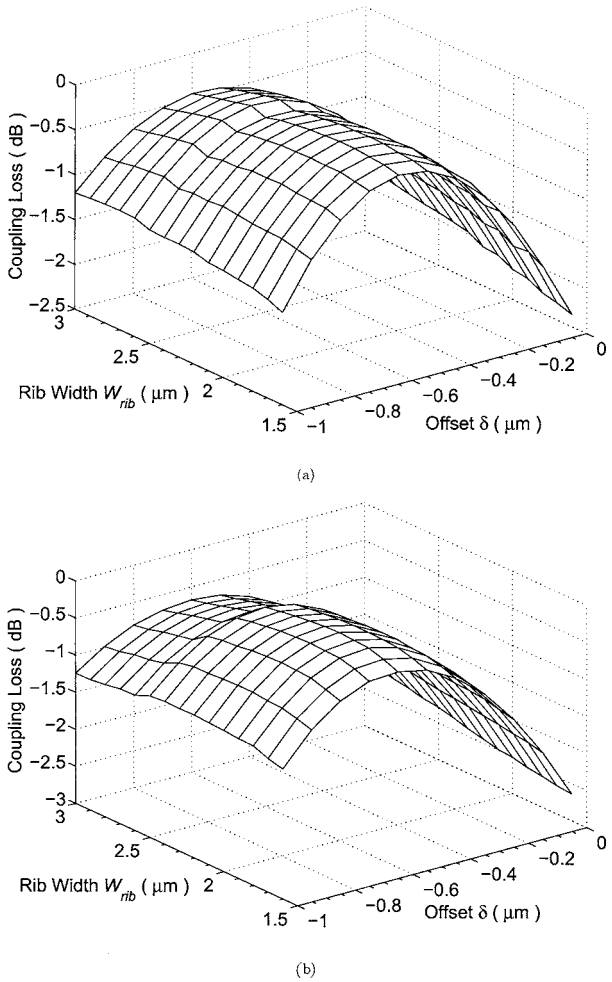


Fig. 8. Coupling loss between the butt-coupled SOI polarization converter and the input and output rib waveguides: (a) TE-polarized input and (b) TM-polarized input.

to 3.0 μm yields, instead, losses of 0.45 dB for an incoming TE mode and 0.68 dB for a TM mode.

5. CONCLUSIONS

We have analyzed two single-section SOI polarization rotators designed to exhibit nearly 100% polarization conversion efficiency. These SOI polarization converters display almost identical efficiency for both TE→TM and TM→TE polarization conversion. A study of fabrication error in these devices demonstrated that the thickness of the outer-slab waveguiding layer is a far more critical parameter than the rib width or height in determining the polarization conversion efficiency, while the refractive index variations resulting from the doping density of the silicon guiding region has little effect on the performance variation. The loss introduced by the butt coupling can be minimized to as low as −0.2 dB by adjusting the displacement between the two waveguide centers. In conjunction with their known wavelength insensitivity, the fabrication tolerance of SOI polarization rotators indicates that these devices can be widely applied in silicon photonics and in DWDM systems.

ACKNOWLEDGMENTS

This work was supported by the Canadian Institute for Photonic Innovations (CIPI) and the Natural Science and Engineering Research Council of Canada (NSERC).

Corresponding author H. Deng can be reached by e-mail at hdeng@engmail.uwaterloo.ca.

REFERENCES

1. R. C. Alferness, "Guided-wave devices for optical communication," IEEE J. Quantum Electron. **QE-17**, 946–959 (1981).
2. I. Kiyat, A. Aydinli, and N. Dagli, "A compact silicon-on-insulator polarization splitter," IEEE Photon. Technol. Lett. **17**, 100–102 (2005).
3. T. K. Liang and H. K. Tsang, "Integrated polarization beam splitter in high index contrast silicon-on-insulator waveguides," IEEE Photon. Technol. Lett. **17**, 393–395 (2005).
4. Y. Shani, R. Alferness, T. Koch, U. Koren, M. Oron, B. I. Miller, and M. G. Young, "Polarization rotation in asymmetric periodic loaded rib waveguides," Appl. Phys. Lett. **59**, 1278–1280 (1991).
5. H. Heidrich, P. Albrecht, M. Hamacherm, H.-P. Nolting, H. Schroeter-Janssen, and C. M. Weinert, "Passive mode converter with a periodically tilted InP/GaInAsP rib waveguide," IEEE Photon. Technol. Lett. **4**, 34–36 (1992).
6. J. J. G. M. van der Tol, J. W. Pedersen, E. G. Metaal, F. Hakimzadeh, Y. S. Oei, F. H. Groen, and I. Moerman, "Realization of a short integrated optic passive polarization converter," IEEE Photon. Technol. Lett. **7**, 893–895 (1995).
7. V. P. Tzolov and M. Fontaine, "A passive polarization converter free of longitudinally-periodic structure," Opt. Commun. **127**, 7–13 (1996).
8. J. Z. Huang, R. Scarmozzino, G. Nagy, M. J. Steel, and R. M. Osgood, Jr., "Realization of a compact and single-mode optical passive polarization converter," IEEE Photon. Technol. Lett. **12**, 317–319 (2000).
9. B. M. A. Rahman, S. S. A. Obayya, N. Somasiri, M. Rajarajan, K. T. V. Grattan, and H. A. El-Mikathi, "Design and characterization of compact single-section passive polarization rotator," J. Lightwave Technol. **19**, 512–519 (2001).
10. N. Somasiri, B. M. A. Rahman, and S. S. A. Obayya, "Fabrication tolerance study of a compact passive polarization rotator," J. Lightwave Technol. **20**, 751–757 (2002).
11. H. El-Refaei and D. Yevick, "An optimized InGaAsP/InP polarization converter employing asymmetric rib waveguides," J. Lightwave Technol. **21**, 1544–1548 (2003).
12. H. El-Refaei, D. Yevick, and T. Jones, "Slanted-rib waveguide InGaAsP–InP polarization converters," J. Lightwave Technol. **22**, 1352–1357 (2004).
13. D. Correia, J. P. da Silva, and H. E. Hernández-Figueroa, "Genetic algorithm and finite-element design of short single-section passive polarization converter," IEEE Photon. Technol. Lett. **15**, 915–917 (2003).
14. H. Deng, D. O. Yevick, C. Brooks, and P. E. Jessop, "Design rules for slanted-angle polarization rotators," J. Lightwave Technol. **23**, 432–445 (2005).
15. C. Brooks, P. E. Jessop, H. Deng, D. O. Yevick, and G. Tarr, "Polarization rotating waveguides in silicon on insulator," in *Proceedings of Integrated Photonics Research Conference (IPR'04)* (Optical Society of America, 2004), paper IFG4.
16. C. Brooks, P. E. Jessop, H. Deng, D. O. Yevick, and G. Tarr, "Passive silicon-on-insulator rotating waveguides," Opt. Eng. (Bellingham) **45**, 044603 (2006).
17. M. Koshiba and Y. Tsuji, "Curvilinear hybrid edge/nodal elements with triangular shape for guided-wave problems," J. Lightwave Technol. **18**, 737–743 (2000).
18. K. Saitoh and M. Koshiba, "Full-vectorial finite element beam propagation method with perfectly matched layers for anisotropic optical waveguides," J. Lightwave Technol. **19**, 405–413 (2001).